

Magnetic structure of CeRhIn₅ as a function of pressure and temperature

A. Llobet,^{1,*} J. S. Gardner,^{2,†} E. G. Moshopoulou,³ J.-M. Mignot,⁴ M. Nicklas,^{1,‡} W. Bao,¹ N. O. Moreno,¹
P. G. Pagliuso,^{1,B} I. N. Goncharenko,⁴ J. L. Sarrao,¹ and J. D. Thompson¹

¹Los Alamos National Laboratory, Los Alamos, New Mexico 87545, USA

²NRC Canada, NPMR, Chalk River Laboratories, Chalk River, Ontario, Canada K0J 1J0

³National Center for Scientific Research "Demokritos," Institute of Materials Sciences, 15310 Agia Paraskevi, Greece

⁴Laboratoire Léon Brillouin (CEA-CNRS), CEA/Saclay, 91191 Gif-sur-Yvette Cedex, France

(Received 30 June 2003; published 13 January 2004)

We report magnetic neutron-diffraction and electrical resistivity studies on single crystals of the heavy-fermion antiferromagnet CeRhIn₅ at pressures up to 2.3 GPa. These experiments show that the staggered moment of Ce and the incommensurate magnetic structure change weakly with applied pressure up to 1.63 GPa, where resistivity, specific heat and nuclear quadrupole resonance measurements confirm the presence of bulk superconductivity. This work places important constraints on an interpretation of the relationship between antiferromagnetism and unconventional superconductivity in CeRhIn₅.

DOI: 10.1103/PhysRevB.69.024403

PACS number(s): 75.25.+z, 71.27.+a, 75.30.-m

I. INTRODUCTION

Heavy-fermion (HF) materials provide an excellent opportunity to investigate the interaction between magnetism and superconductivity (SC). In most HF compounds the magnetic interactions are governed by the hybridization of the *f* electrons and the conduction electrons. This leads to competition between the tendency to order magnetically, favored by the Ruderman-Kittel-Kasuya-Yosida indirect exchange interaction, and the tendency to have a spin-singlet ground state mediated by the Kondo interaction. In these systems superconductivity is found nearby an antiferromagnetic (AFM) phase in the vicinity of a quantum-critical point and the power laws in physical properties below T_C suggest that superconductivity is unconventional.¹ These observations lead to the speculation that strong magnetic fluctuations constitute the quasiparticle pairing mechanism.²⁻⁷ Several families of HF compounds are known where SC does coexist with weak magnetic order [e.g., UPt₃, URu₂Si₂, UNi₂Al₃ (Ref. 1)]. However most of Ce-based heavy-fermion superconductors (HFS) [CeIn₃,^{8,9} CeCu₂Ge₂,^{10,11} CePd₂Si₂,^{12,13} CeRh₂Si₂ (Ref. 14)] display an AFM ground state at ambient pressure and superconduct when external pressure is applied and T_N is driven to 0 K.

A new family of Ce-based compounds, CeMIn₅ ($M = \text{Co, Ir, Rh}$) with Sommerfeld coefficients (γ) of 1000, 750, and 380 mJ mol⁻¹ K⁻², respectively, has recently been added to the list of HFS.¹⁵⁻²⁰ The most notable properties in this series include ambient-pressure magnetic order ($T_N = 3.8$ K) and pressure-induced unconventional SC ($T_C = 2.1$ K at $P = 1.63$ GPa) in CeRhIn₅,^{15,20-23} unconventional ambient-pressure SC in both CeIrIn₅ ($T_C = 0.4$ K) and CeCoIn₅ ($T_C = 2.3$ K) (Refs. 17, 19, and 24) and coexistence of SC and AFM in solid solutions of CeRh_{1-x}A_xIn₅ ($A = \text{Ir, Co}$).^{25,26} The HoCoGa₅-type crystal structure is common to these compounds ($a = b \approx 4.66$ Å and $c \approx 7.51$ Å) (Ref. 27) and consists of alternating layers of CeIn₃ and MIn₂ stacked sequentially along the [001] direction.

Here we focus on CeRhIn₅ which orders at ambient pres-

sure in an incommensurate AFM helical structure²⁸ with a wave vector $q_m = (0.5, 0.5, 0.297)$.²⁹ For $P \geq 1.5$ GPa, the AFM ground state is suppressed and bulk SC is observed below $T_C = 2.2$ K.^{15,20} ¹¹⁵In nuclear quadrupole resonance (NQR) studies on CeRhIn₅ initially reported a decrease with applied pressure of the internal magnetic field (H_{int}) at the In(1) site (located in the CeIn₃ layer) and the authors attributed this decrease either to a reduction of the ordered moment of that Ce or its rotation out of the *a-b* plane with pressure.^{22,23} Recent NQR studies found that AFM coexists homogeneously with SC at a microscopic level in CeRhIn₅ and estimate that, if the ordered moment is reduced with pressure, its value at 1.75 GPa, where AFM coexists with bulk SC, is at most 5% of its ambient pressure value.³⁰ On the other hand, specific-heat measurements on CeRhIn₅ show that the entropy below T_N decreases by about 20% as pressure is raised from 0.3 to 1.32 GPa (Ref. 20) which appears to be inconsistent with the reduction of the ordered moment suggested by NQR results. Neutron-diffraction studies are required for an unambiguous determination of the pressure evolution of the ordered moment and magnetic structure.

An initial neutron-diffraction study under hydrostatic pressure ($P < 0.4$ GPa) on CeRhIn₅ (Ref. 31) revealed no changes in the staggered moment nor T_N within the error bars of the experiment and reported a slight reduction in the incommensurate wave number. Consistent with this first study, more recent neutron-diffraction measurements find essentially no change in the magnetic structure at low pressures.³² However, around 1 GPa, Majumdar *et al.* reported a marked change in the wave vector from (0.5, 0.5, 0.298) to (0.5, 0.5, 0.396) and a 20% reduction of the magnetic moment. They also reported no evidence for AFM order above 1.3 GPa, which contrasts with resistivity, specific-heat, and NQR observations,^{15,20,22,23,30,33} and tentatively ascribe the change in the magnetic structure to a change in the electronic structure under pressure. However, de Haas-van Alphen results show that the topology of the Fermi surface does not change at pressures below 2.0 GPa (Ref. 34) and that there is a steep increase in the cyclotron

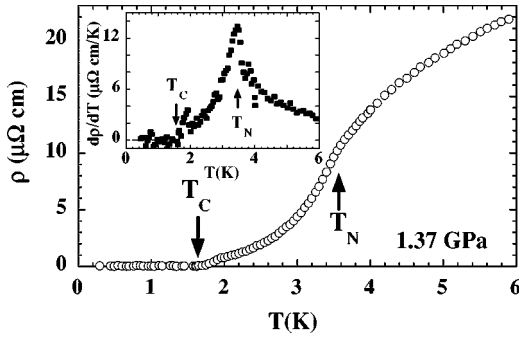


FIG. 1. Temperature dependence of the in-plane resistivity of CeRhIn_5 at $P=1.37$ GPa. The inset shows the derivative of the resistivity where the magnetic and superconducting transitions are clearly indicated.

mass only above 1.6 GPa when SC develops. Additional x-ray-diffraction studies confirm that the CeRhIn_5 crystal structure, except for a small decrease in the cell volume, remains unchanged for pressures up to 2.0 GPa.³⁵ In this work, we have extended the pressure range over which electrical resistivity and neutron-diffraction measurements have been performed on CeRhIn_5 in order to investigate the effect of pressure on the superconducting and magnetic transition temperatures and the evolution of the magnetic structure as pressure approaches and exceeds the critical pressure where the two phases meet.

II. EXPERIMENTAL DETAILS

Single crystals of CeRhIn_5 were grown using the In flux technique.^{36,37} Four-probe ac resistivity measurements, with the current flowing in the tetragonal basal plane, were made on bar-shaped single crystals. A clamp-type cell generated hydrostatic pressures to 2.3 GPa for resistivity measurements using silicon oil as the pressure medium.

Neutron-diffraction experiments were carried out at the C5 and N5 spectrometers at the NRU reactor, Chalk River Laboratories (CRL) as well as at the 6T2 lifting detector diffractometer at the Laboratoire Léon Brillouin, Saclay (LLB). A clamp-type Cu-Be cell³⁸ was used in experiments performed at CRL with Fluorinert-75 as the pressure medium to generate up to 1.8 GPa. Bar-shaped single crystals ($1.3 \times 1.3 \times 10 \text{ mm}^3$) were used to reduce neutron absorption by In and Rh nuclei at CRL. The longest dimension of the crystals was along the $(1\bar{1}0)$ crystallographic axis. The scattering plane was defined to be $(hh\ell)$. In this setup, the applied pressure was determined, within ± 0.1 GPa, by measuring the lattice parameters of a graphite crystal placed behind the sample inside the cell at low temperature. Neutron beams with incident energy of $E_i=35$ meV were produced from a Ge(113) or Be(002) monochromator. Pyrolytic graphite (PG) filters with approximate thickness of 10 cm were placed in the scattered beam to reduce higher order reflections and occasionally a pyrolytic graphite analyzer was used to improve the signal-to-noise ratio.

At LLB, a gasketed sapphire anvil cell was used with a mixture of methanol and ethanol as the pressure transmitting

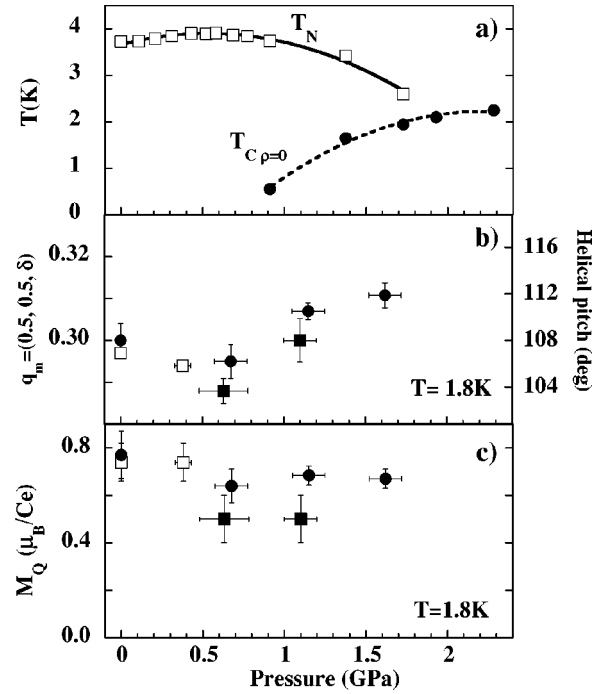


FIG. 2. (a) Temperature-pressure phase diagram for CeRhIn_5 determined by $\rho(T)$ measurements. Open squares correspond to the Néel temperature and solid circles to the temperature at which the resistivity drops to zero. The lines are guides to the eye. (b) Pressure evolution of the antiferromagnetic helical structure characterized by the propagation vector $q_m=(0.5,0.5,\delta)$. (c) Pressure evolution of the estimated Ce staggered moment at $T=1.85$ K of CeRhIn_5 . Filled circles correspond to measurements performed at CRL, filled squares correspond to measurements performed at LLB Saclay, and empty squares correspond to data reported by Bao *et al.*^{29,31}

medium for experiments at 0.63 and 1.1 GPa. Samples, with dimensions $1.3 \times 1.3 \times 0.2 \text{ mm}^3$, were aligned with the $[001]$ crystallographic direction (shortest dimension) vertical. A thin layer of ruby powder was placed on the inner surface of the anvil in order to measure the applied pressure at room temperature using the standard ruby fluorescence technique. This was performed before and after thermal cycling to ensure that pressure was constant throughout the experiment. This technique allows determining the pressure at low temperatures within ± 0.15 GPa. Neutron beams of $E_i=14.81$ meV were produced using a PG(002) monochromator. In both laboratories a top loading He-flow cryostat was used to cool down the pressure cell and sample. Results reported below were obtained on several different single crystals, in different pressure environments and at two neutron sources. The consistency of these results substantiates conclusions drawn from them.

III. RESULTS AND DISCUSSION

We measured electrical resistivity ρ on CeRhIn_5 single crystal at different applied pressures and temperatures from 300 mK to room temperature. A representative plot of $\rho(T)$ is shown in Fig. 1. At 1.37 GPa, signatures for superconduc-

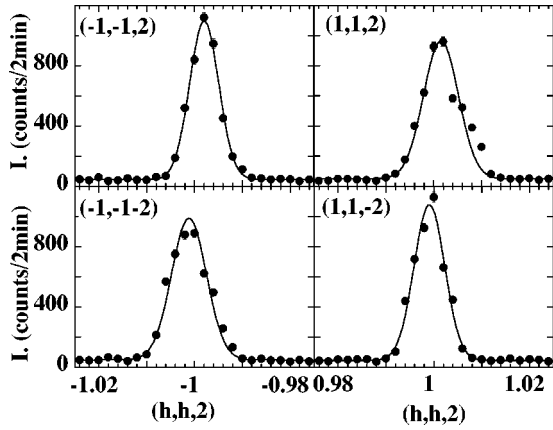


FIG. 3. Elastic q scans through selected nuclear Bragg peaks at $T=1.8$ K and $P=1.15$ GPa.

tivity and antiferromagnetic order are observed in both $\rho(T)$ and its derivative. This crystal has a resistivity ratio $\rho(295 \text{ K})/\rho(1.5 \text{ K})=280$ that is about two times higher than that in a crystal studied by Hegger *et al.*¹⁵ The pressure-temperature (P - T) phase diagram constructed from these $\rho(T)$ measurements is shown in Fig. 2(a). Our results show that the magnetic to nonmagnetic transition is smooth and reveals the existence of a large pressure region of coexisting long-range magnetic order and SC ($0.9 \text{ GPa} \leq P \leq 1.75 \text{ GPa}$). There is a slight increase of T_N with pressure up to about 0.8 GPa and for pressures above this value T_N decreases and a SC ground state develops. This phase diagram is fully consistent with that determined by specific heat²⁰ and NQR (Refs. 22, 23, and 30) and departs from initially reported results.¹⁵

To determine the pressure evolution of the magnetic structure of CeRhIn₅ and particularly the incommensurability parameter (δ) of the magnetic structure [$q_m = (0.5, 0.5, \delta)$] special attention has been paid to the precise alignment of the single crystal since δ depends critically on it. For this reason, systematic checks have been performed during the measurements using $\{1,1,2\}$, $\{0,0,3\}$, and $\{2,2,0\}$ nuclear Bragg reflections. Figure 3 shows typical q scans around a series of $\{1,1,2\}$ reflections at 1.85 K and 1.15 GPa which attest to the quality of the crystal alignment. When changing pressure, the cell and sample were warmed to room temperature before the next pressure was applied. At each pressure, q scans and rocking curves were measured at magnetic and nuclear peaks. Several magnetic reflections, including Friedel pairs, were measured to determine δ more accurately. A set of representative magnetic Bragg peaks is shown in Fig. 4 for $P=1.15$ GPa and $T=1.85$ K. The absence of other commensurate reflections, such as $(0.5, 0.5, 0.5)$, was also systematically verified. From data such as shown in Fig. 4, we obtain the pressure dependence of δ plotted in Fig. 2(b). Our results show that there is no substantial change in the magnetic wave vector $(0.5, 0.5, \delta)$ within the accuracy of these measurements up to pressures of 1.63 GPa. This is qualitatively different from the result reported by Majumdar *et al.*³² At 1.8 GPa, we do not detect any evidence for magnetic scattering for temperatures greater than 1.85 K as shown in Fig. 5. We

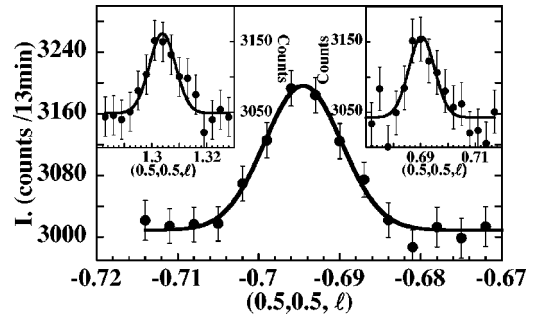


FIG. 4. Elastic q scans around some of the magnetic peaks at $T=1.8$ K and $P=1.15$ GPa.

speculate that the lack of magnetic long-range order at this pressure can be due to the existence of a marginally higher pressure than 1.8 GPa which would drive T_N close to our lowest measuring temperature, in which case the magnetic scattering would be not observable above background scattering from the Be-Cu pressure cell. The possibility that a dramatic change may occur in the magnetic structure between 1.63 GPa and 1.8 GPa giving no magnetic scattering along $(0.5, 0.5, \ell)$ for the ℓ interval reported seems very unlikely but cannot be definitely ruled out.

The temperature dependence of the $(0.5, 0.5, \delta)$ Bragg peak intensity which corresponds to the magnetic order parameter squared is shown in Fig. 6 for $P=0.6$ GPa and 1.1 GPa. It reveals that there is not a significant change in the development of the magnetic order at pressures above and below the pressure where SC starts developing. A tentative fit to $(1 - T/T_N)^{2\beta}$ showed better agreement when $\beta=0.25$, which is consistent with the results reported at ambient pressure.³⁹

To determine the magnetic moment at each pressure, magnetic Bragg peaks were measured at 1.8 K with rocking scans at LLB Saclay and with scans such as those in Fig. 4 at CRL. Magnetic cross sections are derived from integrated intensities with appropriate correction for resolution.⁴⁰ They are normalized to nuclear Bragg peaks to yield values in absolute units. The theoretical cross-section for the AFM spiral model is^{29,41}

$$\sigma(\mathbf{q}) = \left(\frac{\gamma r_0}{2} \right)^2 (M_Q)^2 \frac{1}{4} |f(q)|^2 [1 + (\hat{\mathbf{q}} \cdot \hat{\mathbf{c}})^2], \quad (1)$$

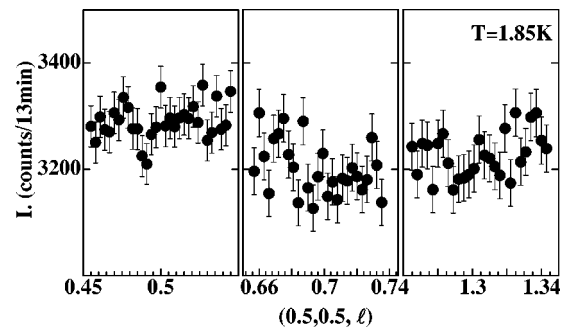


FIG. 5. Selected elastic q scans at $T=1.8$ K and $P=1.8$ GPa not showing any evidence of magnetic scattering.

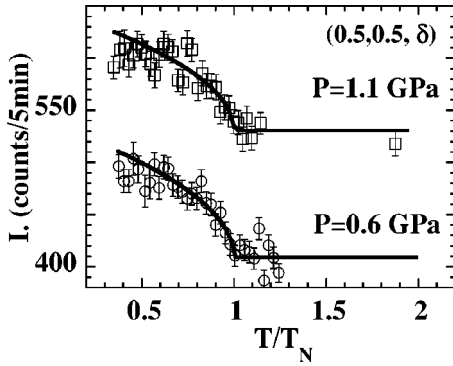


FIG. 6. Temperature dependence of the $(0.5,0.5,\delta)$ Bragg peak intensity at $P=0.6$ GPa and 1.1 GPa (vertical offset added) showing that $T_N(0.6 \text{ GPa}) \sim T_N(1.1 \text{ GPa})$. The solid lines are fits to $(1 - T/T_N)^{2\beta}$ with $\beta=0.25$.

where $f(q)$ is the Ce^{+3} magnetic form factor,⁴² $(\gamma_0 r_0/2)^2 = 0.07265$ barns/ μ_B , and M_Q is the staggered moment of the Ce ion. Figure 2(c) shows the staggered moment of Ce as a function of applied pressure. The staggered magnetic moment of Ce at ambient pressure is $M_Q = (0.8 \pm 0.1) \mu_B/\text{Ce}$, which is consistent with the previously reported value of $M_Q = (0.75 \pm 0.02) \mu_B/\text{Ce}$ and is found to be about 20% smaller than the full moment obtained from crystal-field calculations, which estimate $M_Q = 0.92 \mu_B/\text{Ce}$.⁴³ We attribute the smaller measured value of M_Q to partial Kondo compensation of the moment, an effect neglected in the calculations. Figure 2(c) also shows that there appears to be a slight tendency for M_Q to decrease with pressure (less than 15% decrease at 1.63 GPa compared to ambient pressure).

In earlier resistivity measurements an anomaly at $T=2.8$ K was reported in the pressure range $1.3 < P < 2.0$ GPa on CeRhIn_5 .¹⁵ This anomaly was not observed in specific-heat²⁰ measurements and it is not detected (see Fig. 1) in the higher quality crystals used to construct the phase diagram shown in Fig. 2. We have measured q scans around $(0.5,0.5,\delta)$ at $P=1.63$ GPa for different temperatures in order to determine T_N at this pressure (Fig. 7). Our neutron-diffraction results confirm that magnetic long-range AFM helical order disappears between 2.25 and 2.75 K which is in agreement with the values of T_N

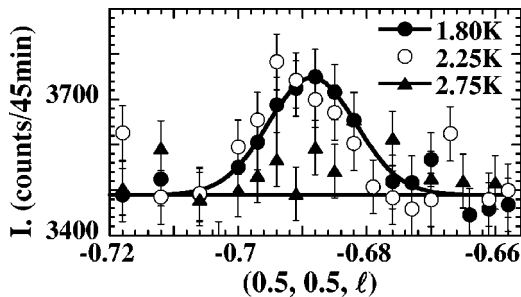


FIG. 7. q scans around $(0.5,0.5,1-\delta)$ magnetic reflection at 1.63 GPa for different temperatures above and below $T_N \approx 2.85$ K using a pyrolytic graphite analyzer to improve the signal-to-background ratio.

extracted from our resistivity measurements [$T_N(1.6 \text{ GPa}) = 2.8$ K] and also with those extracted from NQR measurements.³⁰

For the incommensurate magnetic structure of CeRhIn_5 , the internal magnetic field sensed by ^{115}In -NQR is given by $\mathbf{H}_{int} \propto A_{ab} M_Q \{\sin(q_0 z), \cos(q_0 z), 0\}$, where A_{ab} is the hyperfine coupling between the in-plane In nucleus and each of its four Ce nearest neighbors, M_Q is the ordered moment, and $q_0 = 2\pi\delta/c$.⁴⁴ Our neutron-diffraction experiments show that δ and M_Q change by at most 10% and 15%, respectively, as pressure is raised from atmospheric to 1.63 GPa [Figs. 2(b) and Fig. 2(c)]. These relatively small changes in δ and M_Q are unable by themselves to account for the 80% reduction of H_{int} deduced by NQR measurements. If the Ce moments acquire a component out of the a - b plane as a function of pressure, an apparent decrease of H_{int} would be also observed.²² In such a scenario, additional magnetic diffraction peaks corresponding to a propagation vector different from $(0.5,0.5,\delta)$ would appear and a subsequent reduction of the in-plane component would be observed. We did not observe a large reduction of the in-plane component nor any evidence of magnetic diffraction at $(0.5,0.5,0.5)$ due to an AFM component out of the a - b plane component but we cannot discard magnetic intensity appearing at $(0.5,0.5,0)$. Taken together, our results seem to rule out the canting scenario. An alternative, and more plausible, interpretation of the reduction of H_{int} is that hyperfine coupling decreases with pressure.³¹ Irrespective of the magnitude of H_{int} , NQR measurements³⁰ establish beyond reasonable doubt the coexistence of AFM and bulk SC in CeRhIn_5 at 1.75 GPa. Our diffraction results indicate that $M_Q \approx (0.67 \pm 0.04) \mu_B/\text{Ce}$ at 1.6 GPa and 1.85 K. These results indicate that bulk SC coexists with relatively large-moment AFM order in CeRhIn_5 under pressure.

Unlike UPd_2Al_3 (Ref. 3) where the coexistence of AFM and unconventional SC has been ascribed to the partition of the three U $5f$ electrons into dual roles, magnetic and SC, CeRhIn_5 has only a single $4f$ electron that participates in creating both states. In fact, in most Ce-based HFS the superconducting state develops when T_N is tuned to zero. Indeed CeIn_3 (on which CeRhIn_5 is based) is an example. In CeIn_3 the ordered moment,⁹ and specific-heat anomaly at T_N decrease monotonically towards zero as the critical pressure where SC appears is approached.⁴⁵ We do not understand presently how such a large moment and SC can coexist in CeRhIn_5 . It is as if the $4f$ moments, in some way, also assumed dual character, either in a purely dynamical way as suggested by recent NMR studies⁴⁴ or by segregating into AFM and SC domains. Such segregation, however, also could be dynamic since there is no evidence for additional NQR frequencies.^{22,23,30}

In summary, we have determined a P - T phase diagram from high quality CeRhIn_5 single crystals which shows a broad range of pressures where AFM and SC coexist. In addition, our single-crystal magnetic neutron diffraction studies on CeRhIn_5 find only small changes in the incommensurate magnetic structure and ordered moment as pressure is increased up to 1.63 GPa. These results are consistent with specific-heat measurements but inconsistent with estimates of H_{int} determined by NQR, which we attribute tenta-

tively to a pressure-induced change in the hyperfine coupling. We have not reproduced the observation of a significant change in δ and the absence of AFM at 1.3 GPa reported earlier.³² Most importantly, we have found that compared to other Ce-based HF,¹ the relationship between AFM and SC is qualitatively different in CeRhIn₅ since in this case both relatively large ordered moments and superconductivity exist simultaneously. This will require the development of a new interpretative framework in which the $4f$ electron produces both long-range AFM order and heavy quasiparticles that pair to form the SC ground state.

ACKNOWLEDGMENTS

Work at Los Alamos was performed under the auspices of the U.S. Department of Energy. We would like to thank D. Pines, Ar. Abanov, Z. Fisk, N. J. Curro, and S. Nakatsuji for fruitful discussions. A. Cull, I. Swainson, Th. Beaufils, and J.-L. Meuriot are also thanked for their assistance with the experiments at CRL and LLB. The experiments of E.G.M. at LLB were supported by the European Commission under the Access to Research Infrastructure Action of the Improving Human Potential Program (Contract No. HRPI-CT-1999-0032).

*Electronic address: allobet@lanl.gov

[†]Present addresses: Physics Department, Brookhaven National Laboratory, Upton, New York 11973 and NIST Center for Neutron Research, National Institute of Standards and Technology, Gaithersburg, Maryland 20899-8562.

[‡]Present address: Max Planck Institute for Chemical Physics of Solids, Nöthnitzer Str. 40 01187 Dresden, Germany.

[§]Present address: Instituto de Física “Gleb Wataghin,” UNICAMP, 13083-970, Campinas-SP, Brazil.

¹R.H. Heffner and M.R. Norman, *Comments Condens. Matter Phys.* **17**, 361 (1996); G.R. Stewart, *Rev. Mod. Phys.* **73**, 797 (2001).

²N.D. Mathur, F.M. Grosche, S.R. Julian, I.R. Walker, D.M. Freye, R.K.W. Haselwimmer, and G.G. Lonzarich, *Nature (London)* **394**, 39 (1998).

³N.K. Sato, N. Aso, K. Miyake, R. Shiina, P. Thalmeier, G. Varelogiannis, C. Geibel, F. Steglich, P. Fulde, and T. Komatsubara, *Nature (London)* **410**, 340 (2001).

⁴Z. Fisk, H.R. Ott, and J.L. Smith, in *Proceedings of the Sixth Annual Conference*, Los Alamos, NM, USA, 1986 (unpublished); Z. Fisk, D.W. Hess, C.J. Pethick, D. Pines, J.L. Smith, J.D. Thompson, and J.O. Willis, *Science* **239**, 4835 (1988).

⁵K. Miyake, S. Schmitt-Rink, and C.M. Varma, *Phys. Rev. B* **34**, 6554 (1986).

⁶P. Monthoux, A.V. Balatsky, and D. Pines, *Phys. Rev. Lett.* **67**, 3448 (1991).

⁷P. Coleman and C. Pepin, *Physica B* **312-313**, 383 (2002).

⁸I.R. Walker, F.M. Grosche, D.M. Freye, and G.G. Lonzarich, *Physica C* **282-287**, 303 (1997).

⁹P. Morin, C. Vettier, J. Flouquet, M. Konczykowski, Y. Lassailly, J.M. Mignot, and U. Welp, *J. Low Temp. Phys.* **70**, 377 (1988).

¹⁰D. Jaccard, H. Wilhelm, K. Alami-Yadri, and E. Vargoz, *Physica B* **259-261**, 1 (1999).

¹¹D. Jaccard, K. Behnia, and J. Sierro, *Phys. Lett. A* **163**, 475 (1992).

¹²J.D. Thompson, R.D. Parks, and H. Borges, *J. Magn. Magn. Mater.* **54-57**, 377 (1986).

¹³F.M. Grosche, S.R. Julian, N.D. Mathur, and G.G. Lonzarich, *Physica B* **223-224**, 50 (1996).

¹⁴R. Movshovich, T. Graf, D. Mandrus, J.D. Thompson, J.L. Smith, and Z. Fisk, *Phys. Rev. B* **53**, 8241 (1996).

¹⁵C. Petrovic, E.G. Moshopoulou, M.F. Hundley, J.L. Sarrao, Z. Fisk, and J.D. Thompson, *Phys. Rev. Lett.* **84**, 4986 (2000).

¹⁶C. Petrovic, R. Movshovich, M. Jaime, P.G. Pagliuso, M.F. Hun-

dley, J.L. Sarrao, Z. Fisk, and J.D. Thompson, *Europhys. Lett.* **53**, 354 (2001).

¹⁷C. Petrovic, P.G. Pagliuso, M.F. Hundley, R. Movshovich, J.L. Sarrao, J.D. Thompson, Z. Fisk, and P. Monthoux, *J. Phys.: Condens. Matter* **13**, L337 (2001).

¹⁸G.-q. Zheng, K. Tanabe, T. Mito, S. Kawasaki, Y. Kitaoka, D. Aoki, Y. Haga, and Y. Onuki, *Phys. Rev. Lett.* **86**, 4664 (2001).

¹⁹R. Movshovich, M. Jaime, J.D. Thompson, C. Petrovic, Z. Fisk, P.G. Pagliuso, and J.L. Sarrao, *Phys. Rev. Lett.* **86**, 5152 (2001).

²⁰R.A. Fisher, F. Bouquet, N.E. Phillips, M.F. Hundley, P.G. Pagliuso, J.L. Sarrao, Z. Fisk, and J.D. Thompson, *Phys. Rev. B* **65**, 224509 (2002).

²¹S. Kawasaki, T. Mito, Y. Kawasaki, G.-q. Zheng, Y. Kitaoka, D. Aoki, Y. Haga, and Y. Onuki, *cond-mat/0303123* (unpublished).

²²T. Mito, S. Kawasaki, G.-q. Zheng, Y. Kawasaki, K. Ishida, Y. Kitaoka, D. Aoki, Y. Haga, and Y. Onuki, *Phys. Rev. B* **63**, 220507 (2001).

²³T. Mito, S. Kawasaki, G.-q. Zheng, Y. Kawasaki, K. Ishida, Y. Kitaoka, D. Aoki, Y. Haga, and Y. Onuki, *Physica B* **312-313**, 16 (2002).

²⁴K. Izawa, H. Yamaguchi, Y. Matsuda, H. Shishido, R. Settai, and Y. Onuki, *Phys. Rev. Lett.* **87**, 057002 (2001).

²⁵P.G. Pagliuso, C. Petrovic, R. Movshovich, D. Hall, M.F. Hundley, J.L. Sarrao, J.D. Thompson, and Z. Fisk, *Phys. Rev. B* **64**, 100503 (2001).

²⁶V.S. Zapf, E.J. Freeman, E.D. Bauer, J. Petricka, C. Sirvent, N.A. Frederick, R.P. Dickey, and M.B. Maple, *Phys. Rev. B* **65**, 014506 (2002).

²⁷E.G. Moshopoulou, Z. Fisk, J.L. Sarrao, and J.D. Thompson, *J. Solid State Chem.* **158**, 25 (2001).

²⁸N.J. Curro, P.C. Hammel, P.G. Pagliuso, J.L. Sarrao, J.D. Thompson, and Z. Fisk, *Phys. Rev. B* **62**, R6100 (2000).

²⁹W. Bao, P.G. Pagliuso, J.L. Sarrao, J.D. Thompson, Z. Fisk, J.W. Lynn, and R.W. Erwin, *Phys. Rev. B* **62**, 14 621 (2000); **67**, 099903(E) (2003).

³⁰T. Mito, S. Kawasaki, Y. Kawasaki, G.-q. Zheng, Y. Kitaoka, D. Aoki, Y. Haga, and Y. Onuki, *Phys. Rev. Lett.* **90**, 077004 (2003).

³¹W. Bao, S.F. Trevino, J.W. Lynn, P.G. Pagliuso, J.L. Sarrao, J.D. Thompson, and Z. Fisk, *Appl. Phys. A: Mater. Sci. Process.* **A74**, 557 (2002).

³²S. Majumdar, G. Balakrishnan, M.R. Lees, D. McK. Paul and G.J. McIntyre, *Phys. Rev. B* **66**, 212502 (2002).

³³S. Kawasaki *et al.*, *Phys. Rev. B* **65**, 020504 (2002).

³⁴H. Shishido, R. Settai, S. Araki, T. Ueda, Y. Inada, T.C. Koba-

- yashi, T. Muramatsu, Y. Haga, and Y. Onuki, *Phys. Rev. B* **66**, 214510 (2002).
- ³⁵R.S. Kumar, H. Kohlmann, B.E. Light, A.L. Cornelius, V. Raghavan, T.W. Darling, and J.L. Sarrao, cond-mat/0209005 (unpublished).
- ³⁶E.G. Moshopoulou, Z. Fisk, J.L. Sarrao, and J.D. Thompson, *J. Solid State Chem.* **25**, 158 (2001).
- ³⁷P.G. Pagliuso, C. Petrovic, R. Movshovich, D. Hall, M.F. Hundley, J.L. Sarrao, J.D. Thompson, and Z. Fisk, *Phys. Rev. B* **64**, 100503 (2001).
- ³⁸J.D. Thompson, *Rev. Sci. Instrum.* **55**, 231 (1984).
- ³⁹W. Bao, G. Aeppli, J.W. Lynn, P.G. Pagliuso, J.L. Sarrao, M.F. Hundley, J.D. Thompson, and Z. Fisk, *Phys. Rev. B* **65**, 100505 (2002).
- ⁴⁰M.J. Cooper, *Acta Crystallogr., Sect. A: Cryst. Phys., Diffr., Theor. Gen. Crystallogr.* **A6**, 624 (1968); M.J. Cooper and R. Nathans, *ibid.* **A6**, 619 (1968).
- ⁴¹J.-M. Mignot, F. Bourdarot, A. Llobet, and Ar. Abanov (private communication).
- ⁴²M. Blume, A.J. Freeman, and R.E. Watson, *J. Chem. Phys.* **37**, 1245 (1962).
- ⁴³A.D. Christianson, J.M. Lawrence, P.G. Pagliuso, N.O. Moreno, J.L. Sarrao, J.D. Thompson, P.S. Riseborough, S. Kern, E.A. Goremychkin, and A.H. Lacerda, *Phys. Rev. B* **66**, 193102 (2002).
- ⁴⁴N.J. Curro, J.L. Sarrao, J.D. Thompson, P.G. Pagliuso, S. Kos, Ar. Abanov, and D. Pines, *Phys. Rev. Lett.* **90**, 227202 (2003).
- ⁴⁵G. Knebel, D. Braithwaite, P.C. Canfield, G. Lapertot, and J. Flouquet, *High Press. Res.* **22**, 167 (2002).